The Effect of Turbulence Penetration on the Thermal Stratification Phenomenon Caused by Coolant Leaking in a T-Branch of Square Cross-Section

Young Don Choi†, Seok Woo Hong*, Min Soo Park*

Department of Mechanical Engineering, Korea University, Seoul 136-701, Korea

**Graduate School, Korea University, Seoul 136-701, Korea*

Key words: Thermal stratification, Turbulence penetration, T-branch, Emergency core coolant system

ABSTRACT: In the nuclear power plant, emergency core coolant system (ECCS) is furnished at reactor coolant system (RCS) in order to cool down high temperature water in case of emergency. However, in this coolant system, thermal stratification phenomenon can occur due to coolant leaking in the check valve. The thermal stratification produces excessive thermal stresses at the pipe wall so as to yield thermal fatigue crack (TFC) accident. In the present study, effects of turbulence penetration on the thermal stratification into T-branches with square cross-section in the modeled ECCS are analysed numerically. Standard $k-\varepsilon$ model is employed to calculate the Reynolds stresses in momentum equations. Results show that the length and strength of thermal stratification are primarily affected by the leak flow rate of coolant and the Reynolds number of duct. Turbulence penetration into the T-branch of ECCS shows two counteracting effects on the thermal stratification. Heat transport by turbulence penetration from main duct to leaking flow region may enhance thermal stratification while the turbulent diffusion may weaken it.

Nomenclature

A	: leaked area
A_i	: coefficients of discretization equation
a_i	: covariant basic vector
A^i	: area vector
a^i	: contravariant basic vector
A_{ij}	: area tensor
$C_{\varepsilon 1}, C_{\varepsilon 2}, C_\mu$	: model constants
$\sqrt{g}$	: Jacobian
g_i	: gravitational acceleration in i direction
g^{ij}	: contravariant metrix tensor
G_k	: buoyancy production rate of turbulent kinetic energy
k	: turbulent kinetic energy
L	: length of branch
P_k	: shear production rate of turbulent kinetic energy
Pr	: Prandtl number
Re	: Reynolds number
T	: absolute temperature
T_0	: reference temperature
U_i	: mean velocity component of i direction
$\overline{u_i u_j}$	: Reynolds stress tensor
U^{ξ^i}	: contravariant velocity vector
V_i	: in-leakage velocity
V_m	: bulk mean velocity in a cross-section

† Corresponding author
Tel.: +82-2-3290-3355; fax: +82-2-928-1067
E-mail address: ydchoi@korea.ac.kr

Greek symbols

β : thermal expansion coefficient
Γ^{ij} : diffusion rate tensor
ε : dissipation rate of turbulent kinetic energy
μ : viscosity
μ_t : turbulent viscosity
ξ^i : general coordinate
ρ : density
σ_k, σ_t : turbulent Prandtl number

Subscripts

k : turbulence kinetic energy
m : bulk mean
nb : neighbor point

1. Introduction

On the horizontal part of T-branch in the emergency core coolant system (ECCS) of nuclear reactor, thermal stratification phenomenon can occurr by coolant leaking in the check valve.[1] Continuing existence of thermal stratification and cycling produce excessive thermal stresses on the T-branch to lead to fatigue crack.[2] On December 9, 1987, while nuclear reactor Farley 2 was operating, the licensee noted increased moisture and radioactivity within containment. The source of leakage was a circumferential crack extending through the wall of a short, unisolable section of ECCS piping that is connected to the cold leg of loop in the RCS. On June 18, 1988, same kind of event occurred at the Tihange 1, Westing House-type, pressured-water reactor. Examining the events, NRC (Nuclear Regulatory Commission), published Bulletin 88-08,[3] 88-11,[4] Information notice No. 91-19,[5] 91-28[6] to provide information to addressees about the coolant leaking events and emphasize the need for sufficient examination of unisolable piping connected to the reactor coolant system to assure that there are no rejectable crack or flow indications. Characteristics of the reported events are summarized as follows.

(1) The events occurred due to the leak of coolant in the check valves of ECCS that were connected to the hot legs of RCS.

(2) Turbulence penetration may play an important role to generate the thermal stratification in the T-branch by transporting thermal energy of high temperature from the main pipe to leaking area.

Fig. 1 is the schematic diagram showing the effect of turbulence penetration on the thermal stratification.

NRC emphasized the need for enhanced ultrasonic testing and for experienced examination personnel to detect cracks in piping.

Most of nuclear power plants have followed the recommendations of NRC, but the cause of the events is not yet understood correctly, because only a few theoretical studies have been performed on the thermal stratification phenomena and the corresponding damages[7-9] at the T-branch of ECCS. EPRI (Electric Power Research Institute) proposed to use TASCS program to examine the effect of the leaking flow in the check valve of ECCS on the soundness of piping, but the results are known to be unsatisfactory.

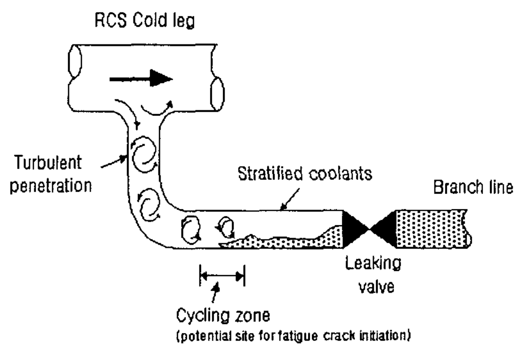

Fig. 1 Schematic diagram showing the effect of turbulent penetration on the thermal stratification.

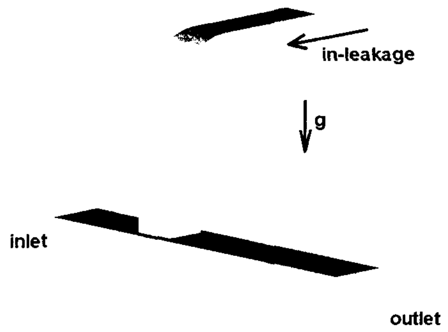

Fig. 2 Schematic diagram of main duct and T-branch with square cross-sections (model of ECCS).

In the present study, to find the primary parameters that affect the thermal stratification occurred in the cold leg of ECCS, numerical analysis is performed for the leak flow in the T-branch of square cross-section. The reason we selected a square sectioned T-branch as shown in Fig. 2 instead of a circular section as the object of numerical analysis is for the thermal stratification by reactor coolant leaking is due to its simple flow passage shape for grid generation and computation. We suppose that the fundamental mechanics between turbulence penetration and thermal stratification in the T-branch may not be different from that of the T-branch of square cross-section and that of circular cross-section.

2. The mathematical and numerical model

2.1 Governing equations

The equations of mean motion for the turbulent flow of water in the square-sectioned main duct and T-branch are conveniently expressed in tensor form:

Continuity

$$\frac{\partial}{\partial x_i}(\rho U_i) = 0 \qquad (1)$$

Mean momentum

$$\frac{\partial}{\partial x_j}(\rho U_i U_j) = -\frac{\partial P}{\partial x_i} + \frac{\partial}{\partial x_j}\left[\mu\left(\frac{\partial U_i}{\partial x_j} + \frac{\partial U_j}{\partial x_i}\right) - \rho\overline{u_i u_j}\right] + g_i(\rho_0 - \rho) \qquad (2)$$

The gravitational term in the right hand side of Eq. (2) is the buoyancy force term. The buoyancy force term can be correlated by the Boussinesq approximation. However, in the computational heat transfers with large temperature change, direct calculations of the term give better results than those obtained using Boussinesq approximation. Therefore, in the present study, the buoyancy force term is calculated directly using the reference density and temperature at the inlet of main duct.

Generally the transportation of the turbulent kinetic energy from the main duct into T-branch by recirculating motion and turbulent diffusion is called turbulence penetration. The transported heat by the turbulence penetration from the main duct to T-branch region has been recognized as the primary cause of the thermal stratification phenomenon due to the coolant leaking in the ECCS.

In order to clarify the effect of turbulence penetration on the thermal stratification in the T-branch of ECCS, turbulence structure in the T-branch should be analyzed. Standard $k-\varepsilon$ model is employed to close the Reynolds stresses in the momentum Eq. (2). In the standard $k-\varepsilon$ model considered, the following closed-form transport equations are solved for turbulent kinetic energy and its dissipation rate:

Turbulence energy

$$\frac{\partial}{\partial t}(\rho k) + \frac{\partial}{\partial x_i}(\rho U_i k) = \frac{\partial}{\partial x_i}\left[\left(\mu + \frac{\mu_t}{\sigma_k}\right)\frac{\partial k}{\partial x_i}\right] + P_k + G_k - \rho\varepsilon \qquad (3)$$

Turbulence energy dissipation rate

$$\frac{\partial}{\partial t}(\rho\varepsilon)+\frac{\partial}{\partial x_i}(\rho u_i\varepsilon)=\frac{\partial}{\partial x_i}\left[\left(\mu+\frac{\mu_t}{\sigma_\varepsilon}\right)\frac{\partial\varepsilon}{\partial x_i}\right] + C_{1\varepsilon}\frac{\varepsilon}{k}(P_k+G_k)-C_{2\varepsilon}\frac{\varepsilon^2}{k} \quad (4)$$

On the other hand, to calculate the heat transport in the T-branch and main duct, the following energy equation is solved.

$$\frac{\partial}{\partial x_i}(\rho U_i T) = \frac{\partial}{x_i}\left[\left(\frac{\mu}{\Pr}+\frac{\mu_t}{\sigma_t}\right)\frac{\partial T}{\partial x_i}\right] \quad (5)$$

where the turbulent viscosity (μ_t), turbulence shear production rate (P_k), turbulence buoyancy production rate (G_k) and turbulence model constants are given by[7]

$$\mu_t=\rho C_\mu\frac{k^2}{\varepsilon},\quad P_k=V_t\left(\frac{\partial U_i}{\partial x_j}+\frac{\partial U_j}{\partial x_i}\right),$$

$$G_k=\frac{\mu_t}{\sigma_t}g_i\beta\frac{\partial T}{\partial x_i},\quad C_\mu=0.09,$$

$$\sigma_k=1.0,\quad \sigma_\varepsilon=1.3,\quad \sigma_t=1.0,$$

$$C_{\varepsilon 1}=1.44,\quad C_{\varepsilon 2}=1.92,\quad \beta=\frac{1}{T}$$

2.2 Discretization of governing equations

Governing equations are transformed from the physical space (x_i) to the computational space (ξ^i). Transformed governing equations into curvilinear coordinate are expressed as the following form.

$$\frac{1}{\sqrt{g}}\frac{\partial}{\partial t}(\sqrt{g}\,\rho\Phi)+\frac{1}{\sqrt{g}}\frac{\partial}{\partial\xi^i}(\sqrt{g}\,\rho U^{\xi^i}\Phi)=\frac{1}{\sqrt{g}}\frac{\partial}{\partial\xi^i}\left(\Gamma^{ij}\frac{\partial\Phi}{\partial\xi^i}\right)+\frac{1}{\sqrt{g}}S \quad (6)$$

where

$$\Gamma^{ij}=\sqrt{g}\,g^{ij}\mu_{eff}=\frac{A^i\cdot A^j}{\sqrt{g}}\mu_{eff}$$

$$U^{\xi^i}=U\cdot a^i$$

$$g^{ij}=a^i\cdot a^j=\frac{A^i\cdot A^j}{\sqrt{g}}$$

$$A^i=\sqrt{g}\,a^i$$

Source term S_j in Eq. (6) includes all the terms except unsteady diffusion and convection terms. By control volume integration, the Eq. (6) can be discretized to

$$A_p U_{ip} = \sum A_{nb}U_{inb}+S_i \quad (7)$$

If the pressure field of the computational domain is known discretized momentum equations can be solved. In the present study, SIMPLE algorithm is employed to revised the pressure field until the convergence is reached. The mass source in pressure correction equation serves as a useful indication of the convergence of the fluid-flow condition. Iteration is continued until the relative overall mass source becomes smaller than 10^{-3}.

2.3 Boundary conditions and wall treatment

Fully developed 363.15 K water flow is given as the inlet boundary condition for main duct. Uniform and steady leak flow of 293.15 K is assumed to take place at the lower part of check valve located in T-branch. Adiabatic condition is imposed as the wall boundary of energy equation. After obtaining the temperature distribution from energy equation, the density, viscosity, thermal conductivity and other properties of water, which are the function of only temperature, are curve fitted by the values of 363.15 K and 293.15 K. For the corresponding Reynolds numbers, fully developed velocity profiles of the square sectioned straight duct were precalculated before the main calculation so as to be used as the inlet velocity conditions of the main duct. Due to the three dimensionality of the computational domain, grid numbers can not be increased to be able to adopt fine grid

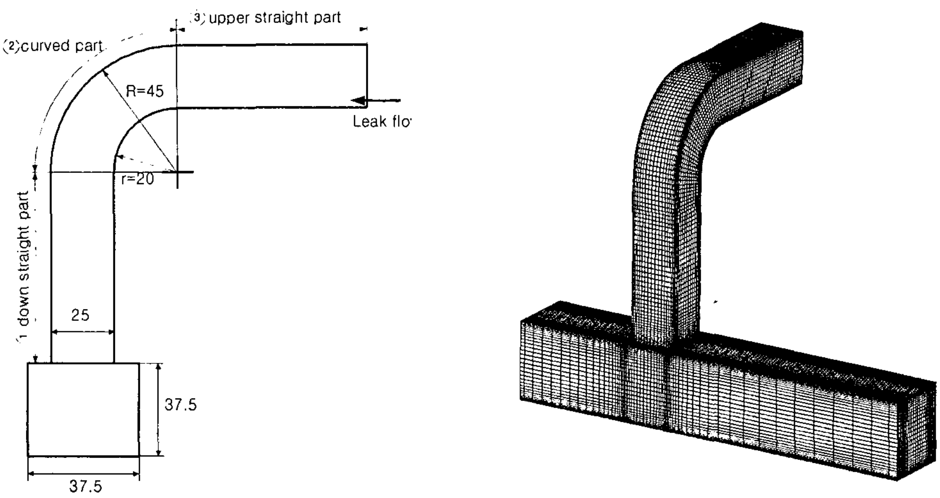

Fig. 3 Dimension and grid generation of T-branch in ECCS.

systems. Therefore, in the present steady, the wall functions modified adaptable to the curvilinear coordinate system were employed.

2.4 Grid generation and computational conditions

The hydraulic diameter (D_H) of main duct is 37.5 mm and that of branch is 25 mm. Table 1 shows the reference condition and the other cases for numerical analysis. The reference Reynolds numbers of main duct and the in-leakage flow rate are selected for the thermal stratification to occur mostly for that condition. Standard grids employed to cover the cross-section of main duct and branch were 43×33 and 21×21 respectively, while the grids in longitudinal direction of main duct and branch were 67 and 121.

3. Results and discussions

Fig. 4, Fig. 5 and Fig. 6 shows the streamlines, temperature and turbulence energy distri-

Table 1 Specifications of reference condition and other conditions for computations

	Inlet			In-leakage			① Down	② Curved		③ Upper
	Re	Velocity [m/s]	In1 [kg/s]	Velocity [m/s]	Area [E-3m^2]	In2 [E-Kg/s]	Length [mm]	r [mm]	R [mm]	Length [mm]
Refence model	57000	0.5	0.675	0.01	0.03435	0.3432	75	20	45	75
A1	34300	0.3	0.405	0.01	0.03435	0.3432	75	20	45	75
A2	114430	1.0	1.35	0.01	0.03435	0.3432	75	20	45	75
A3	228860	2.0	2.7	0.01	0.03435	0.3432	75	20	45	75
B1	34300	0.3	0.405	0.05	0.03435	1.716	75	20	45	75
B2	34300	0.3	0.405	0.1	0.03435	3.432	75	20	45	75
B3	34300	0.3	0.405	0.2	0.03435	6.864	75	20	45	75
B4	34300	0.3	0.405	0.1	0.17175	17.16	75	20	45	75
C1	57000	0.5	0.675	0.01	0.03435	0.3432	150	20	45	150
C2	57000	0.5	0.675	0.01	0.03435	0.3432	225	20	45	225
C3	57000	0.5	0.675	0.01	0.03435	0.3432	300	20	45	300

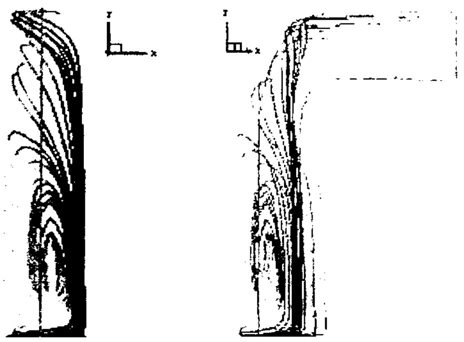

Fig. 4 Streamlines of recirculating flows in the T-branch for the reference condition.

butions in the T-branch of square cross-section for the reference flow condition. The strong recirculating vortex found in the left hand side of Fig. 4 is driven by the forced convection of main duct, and the weak recirculating vortex found in the upper part of right hand side in Fig. 4 is driven by the leak flow. The axes of the two recirculating vortices are orthogonal and meet at the elbow region of T-branch. Thermal and turbulent kinetic energies are transported from the main duct flow to the upper branch region by the interaction of these two orthogonally recirculating vortices. Transfer of thermal energy and turbulence by the interaction of two orthogonally recirculating vortices is of very interesting. Thermal stratification may be enhanced by the thermal energy transport by the recirculating flow, but the turbulence penetration by the interaction of two vortices may reduce the thermal stratification by increasing the thermal diffusion in the upper part of branch.

Variation of the maximum wall temperature

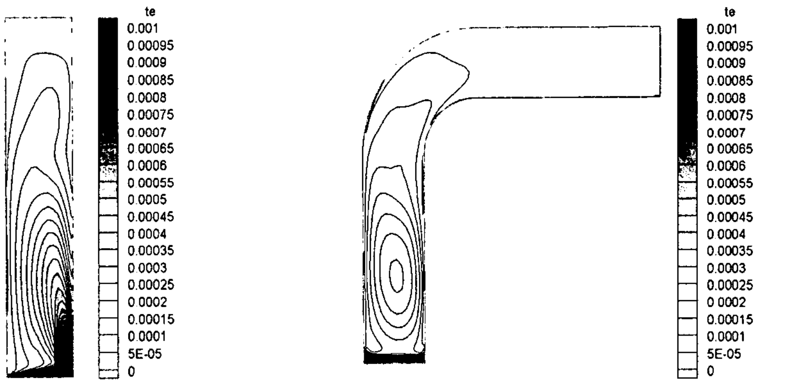

Fig. 5 Turbulence kinetic energy distribution [m^2/sec^2] in the T-branch for the reference condition.

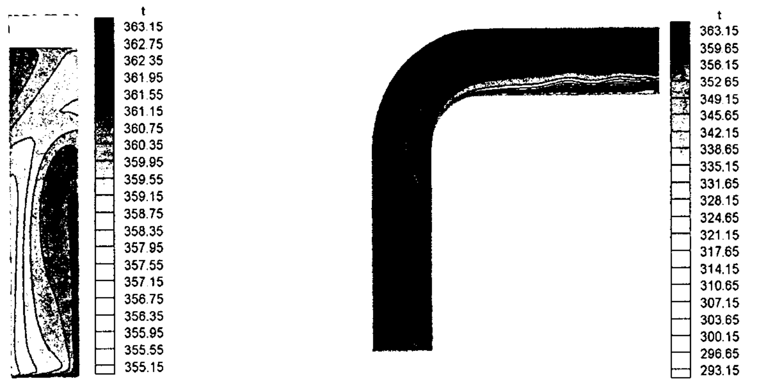

Fig. 6 Temperature distribution [K] in the T-branch for the reference condition.

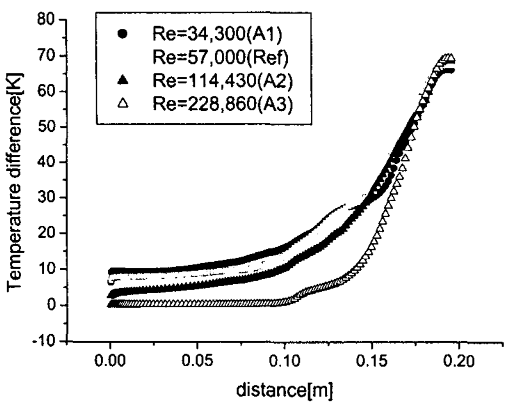

Fig. 7 Variation of maximum wall temperature differences with respect to the distance from main duct.

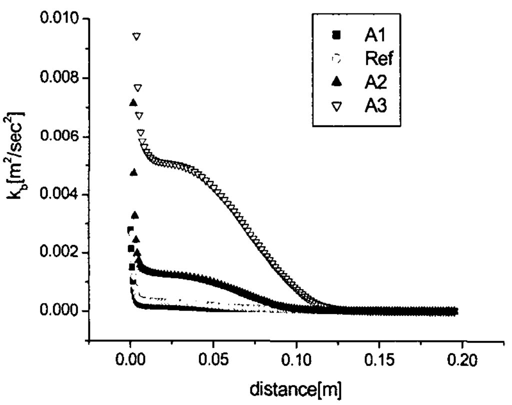

Fig. 8 Variation of bulk mean turbulent kinetic energy with respect to Reynolds number.

difference and the bulk mean turbulent kinetic energy for various Reynolds numbers in the cross-sections of T-branch are compared in Fig. 7 and Fig. 8. The maximum wall temperature difference, which indicates the strength of thermal stratification, decreases according to the increase in Reynolds number. However bulk mean turbulent kinetic energy increases sharply with the increase of Reynolds number in the main duct. It is due to the increase in the strength of primary vortex driven by the main duct flow. Decrease in maximum wall temperature difference in accord with the increase of Reynolds number is relevant to the increased

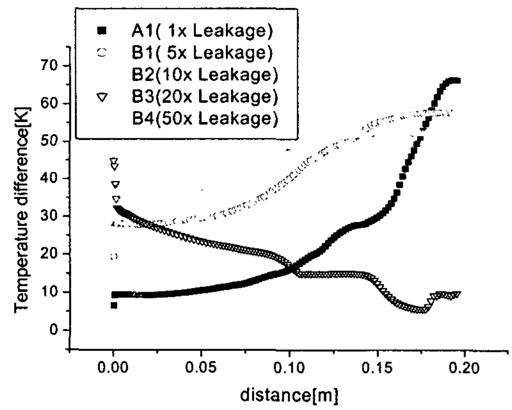

Fig. 9 Variation of maximum wall temperature differences with respect to leak flow rate.

bulk mean turbulence kinetic energy in the T-branch region. The increased turbulence kinetic energy may enhance the thermal mixing to reduce the temperature inhomogeneity in the T-branch region.

Fig. 9 shows the variation of maximum wall temperature difference with respect to leak flow rate. According to the increase of leak flow rate up to 10 times of the reference condition, the length and strength of thermal stratification decrease gradually. However, if the leak flow rate increases over 20 times of the reference condition, the thermal stratification disappears entirely in the upper part of T-branch while it is found in the lower part of T-branch. In this state, leaking flow can not form the wall jet mandatory for the generation of thermal stratification.

Fig. 10 shows the temperature distributions and secondary flow vectors at the three cross-sections in the T-branch. In Fig. 10 (a), where is the nearest cross-section from the in-leakage place, thermal stratification is clearly shown and small vortices are also formed in the lower part of duct. This vortices may be generated by the flow instability induced by the high shear between stagnant fluid and leaking wall jet flow. Fig. 10 (b) is the cross-sectional view at the 37.5 mm away from the in-leakage sec-

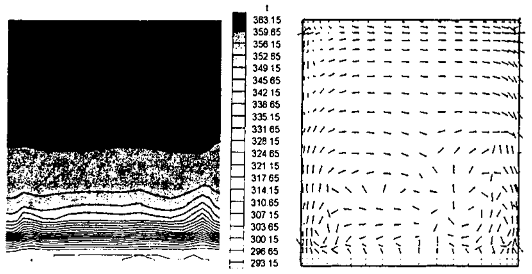

(a) Just before in-leakage

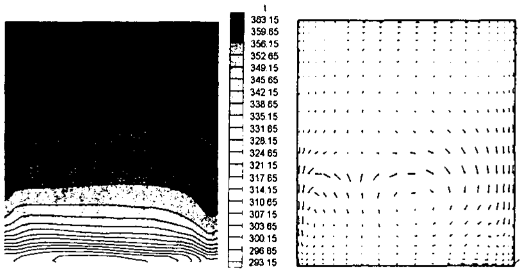

(b) 37.5 mm from in-leakage

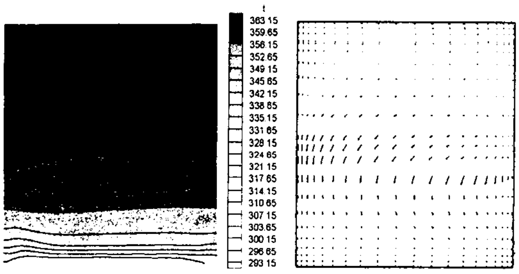

(c) 75.0 mm from in-leakage

Fig. 10 Temperature distribution and secondary flow vectors at the section.

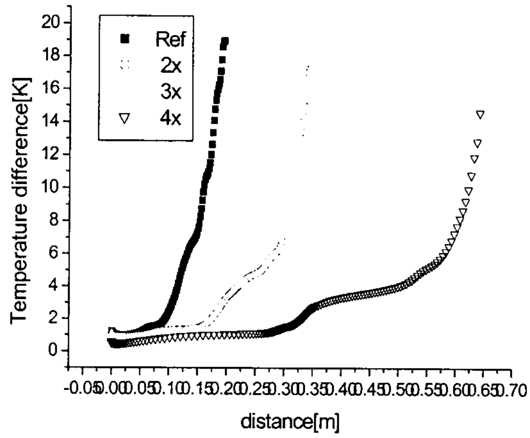

Fig. 11 Variation of maximum wall temperature differences with respect to the length of branch.

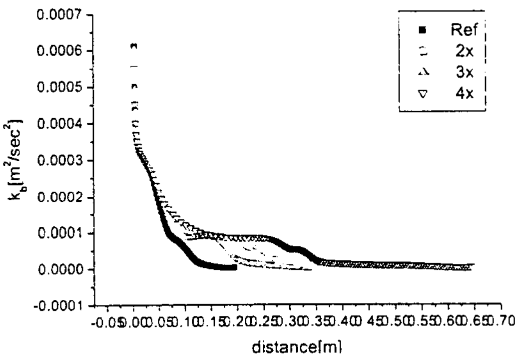

Fig. 12 Variation of bulk turbulence kinetic energy with respect to the length of branch.

tion. This comes under the central part of horizontal region of T-branch. Thermal stratification is weakened, but the secondary vortices are developed more clearly. The cross-sectional view at the 75 mm away from the in-leakage section where is the elbow region, is shown in Fig. 10 (c). Thermal stratification is more weakened, but the secondary vortex flow form a large swirling motion. This is due to the influence of convection in the main duct flow.

The effect of the length of T-branch on the thermal stratification is also investigated in the present study. Fig. 11 and Fig. 12 show the distributions of maximum wall temperature difference and bulk mean turbulent kinetic energy with respect to the length of T-branch. Turbulence penetration increase with the increase in the length of T-branch, while the maximum wall temperature differences decrease with the increase in the length of T-branch.

Primary concern in the thermal stratification analysis of the T-branch in ECCS is how to relieve the thermal stratification in the case of check valve leaking. We suppose that the gradient of T-branch may affect the strength of thermal stratification. Therefore we investigate

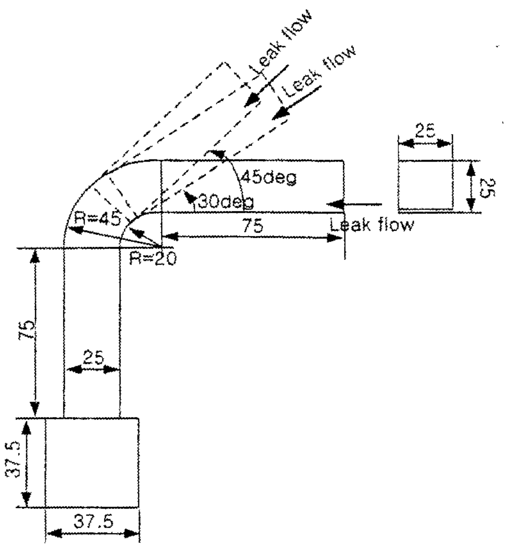

Fig. 13 Schematic diagram showing the inclination of T-branch in ECCS.

the effect of the gradient of T-branch on the thermal stratification by inclining the branch angles to 30° and 45° as shown in Fig. 13.

Distribution of bulk mean temperature and maximum wall temperature difference for the two inclination angles are shown in Fig. 14 and Fig. 15. The figures show that the thermal stratification can be reduced significantly inclining the T-branch angle to 30° and 45°.

4. Conclusions

In the present study, the following conclusions are drawn from the numerical analysis of convective heat transfer in the T-branch of ECCS with variation of Reynolds number, leak flow rate, length of branch and inclination angle of branch.

(1) The recirculating flows driven by main duct flow and leaking wall jet flow meet at the elbow region with orthogonal axes so that turbulence and thermal energies are transported from the main duct to the upper T-branch region by the interaction of the two recirculating vortices.

(2) As with the increase of Reynolds number, turbulence penetration length increases so as to reduce the thermal stratification by enhancing the thermal mixing between leaking flow and stagnant fluid.

(3) There exists the leak flow rate that maximizes the thermal stratification.

(4) At the nearest cross-section from the in-leakage place, small vortices are formed in the lower part of branch duct. This vortices may be generated by the flow instability induced by the high shear between stagnant flow and leaking wall jet flow. High shear between stagnant

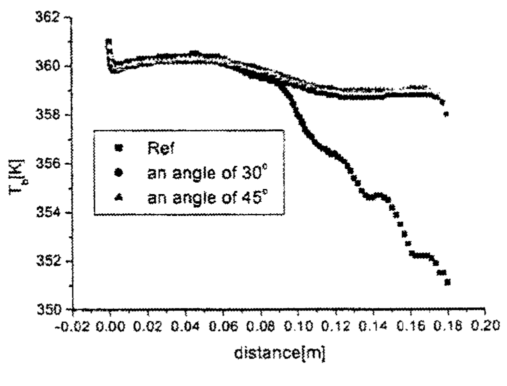

Fig. 14 Variation of bulk temperature with respect to the inclination angle of T-branch.

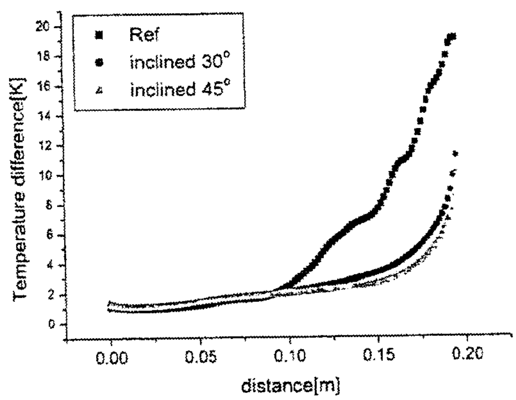

Fig. 15 Variation of maximum wall temperature difference with respect to the inclination angle of T-branch.

fluid and leaking wall jet induces flow instability to generate secondary flow vortices in the cross-sectional plane of T-branch.

(5) Inclining the T-branch angle to 30° and 45°, thermal stratification can be reduced significantly.

Acknowledgement

Present study was performed with the support of Electrical Engineering and Science Research Institute (2000-011).

References

1. EPRI, 1994, Thermal Stratification Cycling and Striping (TASCS), TR-103581.
2. NRC, 1988, Thermal Stress in Piping Connected to RCS, NRC Bulletin 88-08.
3. NRC, 1991, Steam Generator Feedwater Distribution Piping Damage, NRC Information Notice No. 91-19.
4. Hahn, K. S., Kim, S. T., Park, K. S., Chang, K. S. and Choi, S. N., 1998, Fatigue safety analysis on the crack of pressurizer nozzle in nuclear power plant, Transaction of KSME, A, Vol. 22, No. 6, pp. 1123-1133.
5. Park, M. H., Kim, K. C., Noh, H. K. and Kim, K. H., 2000, Numerical study on the thermal mixing flow of cold leg during high pressure safety injection after loss of coolant accident, Proc. of the First National Congress on Fluids Engineering, September, Muju. Korea, pp. 475-478.
6. Kim, J. H., Ridt and Deardorff, A. F., 1993, Thermal stratification and reactor piping integrity, Nuclear Engineering and Design, Vol. 139, pp. 83-95.
7. NRC, 1988, Pressurize Surge Line Thermal Stratification, NRC Bulletin 88-11.
8. Johnson, R. W., 1984, Turbulent Convecting Flow in a Square Duct with a 180 Bend, an Experimental and Numerical Study, Ph. D. Thesis, UMIST.
9. Kim, W. K., 1997, Experimental and Numerical Steady on the Characteristics of Turbulent Flow in the Variable Rectangular Cross-Sectioned 180° Bends, Ph. D. Thesis, Korea University.
10. Lim, H. Y., 2003, Numerical Investigation of Developing Turbulent Heat Transfer to Supercritical Carbon Dioxide Flows Through a Square Duct, Master Thesis, Korea University.